Enhanced Detection and Characterization of Human Targets via Non-Linear Phase Modeling

Sevgi Z. Gürbüz and Douglas B. Williams
School of Electrical and Computer Engineering
Georgia Institute of Technology
Atlanta, GA, USA
sevgi@alum.mit.edu, dbw@ece.gatech.edu

William L. Melvin
Georgia Tech Research Institute
Georgia Institute of Technology
Atlanta, GA, USA
bill.melvin@gtri.gatech.edu

***Abstract*—Many current radar-based human detection systems employ some type of Doppler or Fourier-based processing, followed by spectrogram and gait analysis to classify detected targets. However, Fourier-based techniques inherently assume a linear variation in target phase over the aperture, whereas human targets have a highly nonlinear phase history. This mismatch leads to significant loss in SNR and integration gain. In this paper, two novel human-modeling based non-linear phase detectors are presented. The first (ONLP) computes maximum likelihood estimates of unknown parameters of a model of the human torso response, while the second (EnONLP) stores the expected returns of a 12-point model for each combination of model parameter values in a dictionary and uses orthogonal matching pursuit to find the optimal sparse approximation to the data. The performance of ONLP, EnONLP, and conventional STAP is compared and application to target characterization discussed.**

I. Introduction

The problem of human detection with radar may be broken down into two key tasks: 1) detecting the presence of a target, and 2) deciding whether or not the target detected is human. Much of current research has focused on the latter, overlooking the inherent SNR losses incurred when conventional, linear-phase detectors are applied to human targets. In fact, human targets have a highly non-linear phase history, made unique by the characteristic periodicities of bipedal motion, and differentiable from that of even other animals [1]. This work aims to exploit the results of human modeling and gait analysis to design detectors specifically tailored to approximate as closely as possible the expected return from a human target.

Two approaches are considered. The first is an optimized non-linear phase (ONLP) detector [2-4] that computes maximum likelihood estimates of the unknown parameters in a sinusoidal approximation to the human torso response. The second is an enhanced ONLP (EnONLP) detector that numerically stores the complete modeled human response in a dictionary and uses orthogonal matching pursuit to find the optimal sparse approximation to the received radar data. Results show that both approaches offer significant improvement of detection performance in clutter over conventional STAP, while the EnONLP algorithm also offers a framework for further characterizing detected targets.

II. Signal Modeling

Consider a radar antenna transmitting a series of chirped pulses at constant intervals in time and space while moving along a straight path. In general, the total received signal is comprised of the received radar return plus clutter and noise.

In this work, noise is modeled as complex white Gaussian distributed, while clutter is modeled by a generic physical model that computes the sum of all the clutter returns from a ring of scatterers located at a fixed range, R_c, from the radar.

A. Human Radar Return

A human is a complicated target because of the intricate motion of body parts moving along different trajectories at different speeds. In this work, the human body is divided into twelve basic body parts: the head, upper arms, lower arms, torso, thighs, lower legs and feet - each modeled as a point target located at the center of the body part.

The time-varying position of each point target may be computed using the kinematic model of a walking human developed by Thalmann [5]. The equations for the motion of the spine and charts of the time-varying joint angles may be combined with data on the dimensions of the human body to compute the time-varying positions of each body part.

Exploiting the work of Geisheimer [6] and Van Dorp [7], who showed that that the principle of superposition could be applied to human modeling, the total human return is

$$s_h(n,t) = \sum_{i=1}^{12} a_{t,i}\, rect\left(\frac{\hat{t} - t_{d,i}}{\tau}\right) e^{j[-2\pi f_c t_{d,i} + \pi\gamma(\hat{t} - t_{d,i})^2]}, \quad (1)$$

where the time t is defined as $t = T(n-1) + \hat{t}$ in terms of the pulse repetition interval (PRI), T, the pulse number, n, and the time relative to the start of each PRI, $\hat{t}$; $a_{t,i}$ is the amplitude as given by the radar range equation; τ is the pulse width; c is the speed of light; γ is the chirp slope; f_c is the transmitted center frequency; and $t_{d,i}$ is the round trip time delay between antenna and each body part.

The slow-time, fast-time data matrix is pulse compressed so that the peak occurs at the range bin in which the target is present. Taking a slice across slow-time at the range bin of the peak output,

$$x_p[n] = \sum_{i=1}^{12} a_{t,i} \tau e^{-j\frac{4\pi f_c}{c} R_{d,i}}, \qquad (2)$$

where $R_{d,i}$ is the range from the antenna to each body part.

Although of limited value for classifying these targets, one way of visualizing the human return is via spectrograms, computed from the fast Fourier transforms (FFT) of short, overlapping time segments taken from the slow-time slice in (2), as illustrated in Fig. 1. The strongest return is received from the torso, while the feet appear with the largest amplitude oscillation. This signal structure is unique to humans and exploited in our proposed detector design.

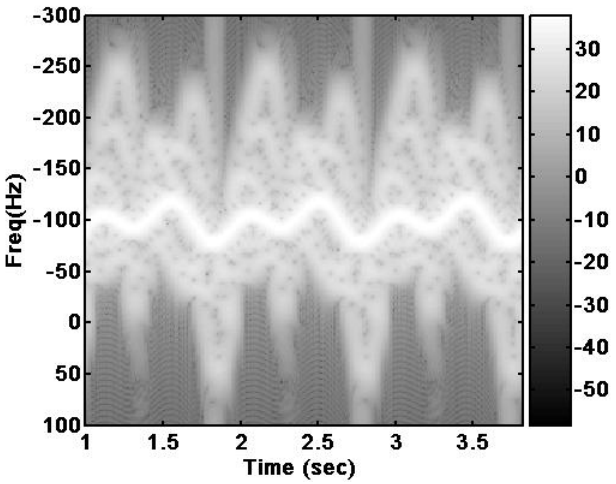

Figure 1. Example human spectrogram.

The multi-channel formulation of (2) may be obtained by incorporating the time delay Δt in the radar return between adjacent elements of the uniform array $\Delta t = d\sin(\phi)/c$, where d is the inter-element spacing, so that the target's contribution to the array's space-time snapshot is

$$\boldsymbol{\chi}_t = \left[\mathbf{x}_p \circ \mathbf{b}_t(\varpi_t)\right] \otimes \mathbf{a}_s(\upsilon_t), \qquad (3)$$

where $\boldsymbol{a_s}$ is the target's spatial steering vector, $\boldsymbol{b_t}$ is the target's temporal steering vector, the spatial frequency υ_t is $f_c nd\sin(\phi)/c$, ϖ_t is the target Doppler shift normalized by the pulse repetition frequency (PRF), and $\circ$ represents the Hadamard product.

B. Inherent SNR Loss

The FFT used in Doppler processing leads to maximum output SNR when the inputs likewise exhibit constant amplitude and linear phase variation over the aperture. However, the phase history of a human target can be highly nonlinear, resulting in an inherent SNR loss when processed by a linear-phase filter, such as the FFT. As shown in Fig 2., collecting data over a longer dwell is not a remedy, as the SNR loss, as shown by the difference between the curves for the ideal, clairvoyant detector and FFT, simply increases with dwell.

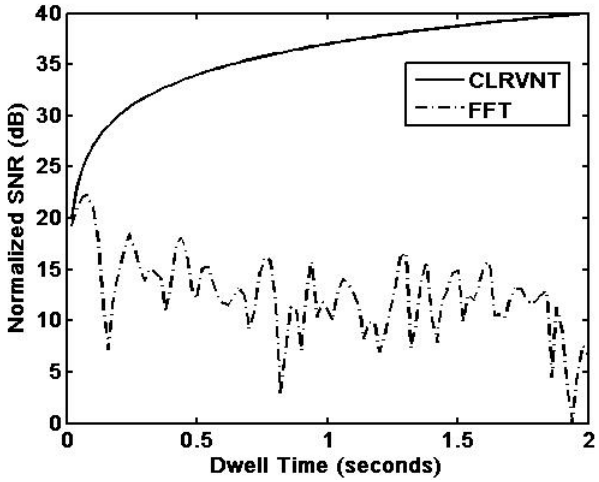

Figure 2. Output SNR variation over dwell time normalized by input SNR for a typical target phase history [4] © IEEE.

III. Parameter Estimation-Based ONLP

The human-model based expression for the target return in (2) is a very good approximation to the true target signal, **s**; however, this model is much too complicated for use as an effective matched filter. The model contains over 24 unknown parameters and most of the kinematic expressions used to compute the time-varying range of each body part are not presented in closed form, but rather as graphs, which must be combined with other charts or equations to derive the time-varying position [5]. The range term in (2) can be simplified by assuming motion along a straight line and fixed angle, θ.

If we define $\boldsymbol{r_I}$ as the vector from the antenna to the target's initial position and $\boldsymbol{r_N}$ as the vector from the antenna to the target's final position, then the vector $\boldsymbol{h}$ between the

initial and final target locations represents the human motion component. Using the law of cosines,

$$\left|\mathbf{r}_N\right|^2 = \left|\mathbf{r}_1\right|^2 + \left|\mathbf{h}\right|^2 - 2\left|\mathbf{r}_1\right|\left|\mathbf{h}\right|\cos\theta \qquad (4)$$

Assuming $\left|\mathbf{h}\right| << \left|\mathbf{r}_1\right|$, and $\sqrt{1+x} \approx 1 + x/2$ for small x,

$$\left|\mathbf{r}_N\right| \approx \left|\mathbf{r}_1\right| - \left|\mathbf{h}\right|\cos\theta . \qquad (5)$$

Moreover, because the impact of phase mismatch is much more significant than that of amplitude mismatch, we approximate $a_t\tau \approx A / r_b^2$ for each body part. Thus, (2) may be written as

$$x_p[n] \approx \frac{A}{r_b^2}\sum_{i=1}^{12} e^{-j\frac{4\pi f_c}{c}(r_i - h_i\cos\theta)} . \qquad (6)$$

where r = $|\mathbf{r}_1|$ and h = $|\mathbf{h}|$.

The model can be further simplified by considering the torso response only, which is significantly stronger than the remaining eleven body parts. Approximating the torso motion with a sinusoidal function, the ONLP approximation in terms of generic parameters may be written as

$$x_p[n] \approx x_{onlp}[n] = \frac{A}{r_b^2} e^{j(Mn + C_1 + C_2\cos(C_3 n + C_4))} \qquad (7)$$

with M, the slope proportional to Doppler frequency; C_1, a factor dependent upon range; C_2, the amplitude of torso motion; C_3, torso frequency; C_4, torso phase; and A, the amplitude as defined in the range equation. These variables are unknown model parameters over which the matched filter response will be optimized.

MLEs of the unknown parameters can be computed for the case of complex Gaussian noise. However, these estimates cannot be computed in closed form. Instead, a system of four non-linear equations with four unknowns is obtained, solvable using numerical iteration. The MLEs obtained are then substituted back into (4) and used to compute the the Adaptive Matched Filter detection test [8].

IV. Dictionary Search-Based EnONLP

The EnONLP method overcomes the difficulty of obtaining good parameter estimates in clutter by storing the expected target return for each possible value of any unknown parameters in a dictionary. In EnONLP, there is no need to limit our model to just the torso response or to simplify the Thalmann equations, as the numerical values are directly stored and used in the algorithm. Thus, the more accurate model in (6) is applied, yielding the additional advantage of possessing physically-relevant unknowns constrained over known finite intervals. Orthogonal matching pursuit is then used to search the dictionary for linear combinations of target responses that best match the measured data.

The dictionary is created by discretizing the range of possible parameter values into a finite number of samples for each parameter. Define $\boldsymbol{\xi} = \begin{bmatrix} v & HT & \phi & \theta & r \end{bmatrix}$ as the vector of unknown parameters. For each possible combination of parameters, $\boldsymbol{\xi}_\mathbf{j}$, the corresponding target return model is computed and stored as an entry in a dictionary (D) of size MN x Q

$$\boldsymbol{\mathcal{D}} = \left[\hat{\boldsymbol{\chi}}_{\mathbf{EnONLP}}(\xi_1) \quad \cdots \quad \hat{\boldsymbol{\chi}}_{\mathbf{EnONLP}}(\xi_j) \quad \cdots \quad \hat{\boldsymbol{\chi}}_{\mathbf{EnONLP}}(\xi_Q)\right] \qquad (8)$$

If multiple targets are present in the data, a linear combination of dictionary entries will best represent the received data. Orthogonal matching pursuit (OMP) [9] is a robust version of a number of sparse approximation techniques, such as basis pursuit or matching pursuit, which may be applied to solve this problem. First, an optimal, fully-adaptive space-time filter is applied to the data to mitigate the affect of clutter. Thus, the residual of the OMP algorithm is initialized to $\mathbf{r_0} = \mathbf{R_I^{-1}}\boldsymbol{\chi}$, where $\mathbf{R_I}$ is the interference covariance matrix and $\boldsymbol{\chi}$ is the space-time snapshot of the data. The dictionary entry for which the projection onto the residual is maximized,

$$\hat{\boldsymbol{\chi}}_{optimal} \rightarrow \max\left\{\mathbf{r_0^H}\boldsymbol{\mathcal{D}}\right\}, \qquad (9)$$

is tested for the presence of a target using the Adaptive Matched Filter detector [9]. If a target is present, then the entry index is stored in a vector $\boldsymbol{\eta}$ and the coefficient vector $\boldsymbol{C}$ that solves the least squares problem

$$\min\left\|\mathbf{R_I^{-1}}\boldsymbol{\chi} - \sum_{j=1}^{t} C(\eta_j)\hat{\boldsymbol{\chi}}_{\mathbf{EnONLP}}(\eta_j)\right\|_2 \qquad (10)$$

is computed. The residual is then updated by subtracting out the components already found, and the procedure is repeated until no more components yield a detection.

Thus, unlike the parameter estimation-based ONLP, the EnONLP algorithm is also able to determine the total number of *resolvable* human targets that reside within a range bin. Targets with close azimuth angles will still be successfully detected but identified as a single target. Furthermore, note that this procedure yields additional information about the detected target, as the parameters used to generate the dictionary entries found to comprise the signal are known. The accuracy of obtained estimates is limited by the fineness in the discretization of the parameter space and by any modeling errors.

V. PERFORMANCE

Detector performance is evaluated by comparing the receiver operating characteristics (ROC) for the EnONLP detector with that of ONLP and fully adaptive, optimum STAP in simulated data of a 5-channel radar with characteristics shown in Table I, chosen as being typical of a representative radar system.

TABLE I

Parameters	Value	Parameters	Value
Pulses #	500	PRI	0.2 ms
Center Freq.	1 GHz	Pulse Width	40 μs
Samp Freq.	20 MHz	Trans. Power	1.8 kW
Bandwidth	10 MHz	Nom. Range	8,760 m

The dictionary used by the EnONLP algorithm is generated by discretizing the unknown velocity at 0.1 m/s increments between 1.5 m/s and 2.7 m/s, and the unknown angles at 5 degree intervals over 360°, for a dictionary of 936 entries. Dictionary size is minimized by storing data for only one channel, using convolution instead of multiplication in (9) to avoid storing phase (range) information, and generating all entries for a fixed-size human, in this case, an average male. Thus, an increase in computational load is traded off for savings in memory.

ROC curves for the EnONLP, ONLP, and STAP detectors are shown in Fig. 3 and Fig. 4 for an average-sized male walking at a 45° angle relative to the x-axis with a speed of 2 m/s. The proposed EnONLP detector exhibits the best performance with a P_D of 0.79 at a P_{FA} at 10^{-6}, steadily increasing as the P_{FA} increases, with the other methods matching performance only when the P_{FA} has risen to 0.01. As the clutter-to-noise ratio (CNR) increases to beyond 15 dB, the other methods exhibit a sharp drop in detection rate, whereas EnONLP is able to maintain good performance.

The EnONLP framework has the additional advantage of being able to detect the number of human targets present in a single range bin, as well as extract an estimate of the modeled parameters for each target. If models for other non-human targets are also included in the dictionary, then EnONLP may also be exploited as a target classifier.

Consider a scenario in which a vehicle, a tall male with thigh height (HT) of 1 meter, and a small female with a thigh height of 0.74 meters are all moving within a single range gate in clutter with an SINR of 20 dB. The vehicle is modeled as a point target with a reflection 10 dB stronger than the male target. Additional scenario parameters are provided in Table 2. Thus, the dictionary is augmented with entries generated from discretized linear spatial and temporal steering vectors. The EnONLP algorithm was able to successfully detect all targets, with model parameter estimates as shown in Table II.

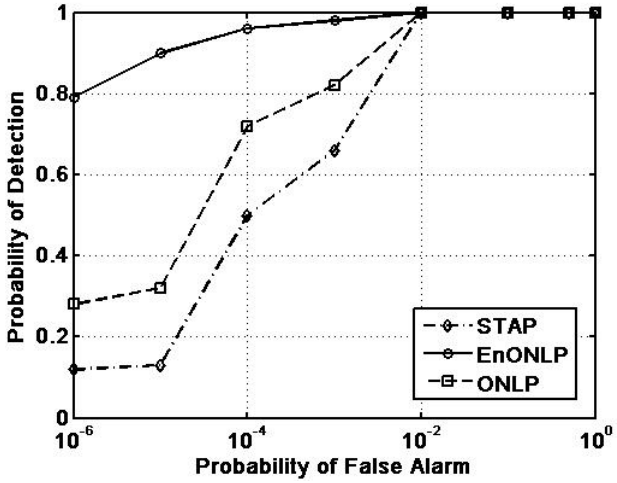

Figure 3. P_D v P_{FA} for a human target with SNR = 0 dB and CNR = 20 dB.

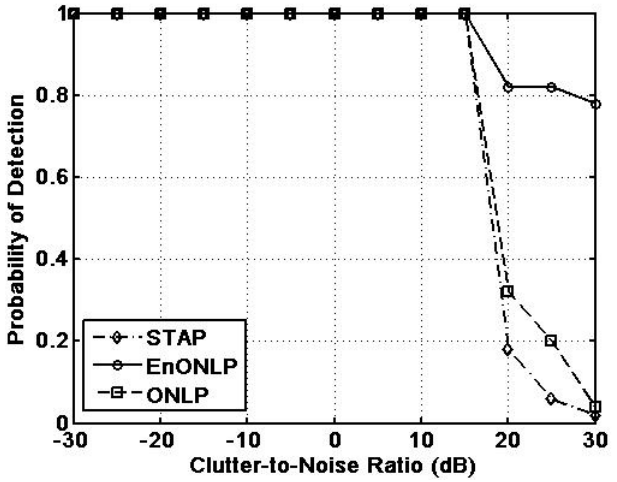

Figure 4. P_D v CNR for a human target with SNR = 0dB and $P_{FA} = 10^{-6}$.

TABLE II

	TRUE		DETECTED	
	Male	Female	Male	Female
Azimuth	60°	-30°	65°	-30°
Direction	15°	30°	15°	35°
Velocity	2 m/s	2.4 m/s	2 m/s	2.3 m/s
	Vehicle		Vehicle	
Azimuth	37°		37°	
Rad. Vel.	14 m/s		14 m/s	

The classification performance of the EnONLP algorithm may be further quantified by considering the confusion matrix shown in Table III, which shows the detection results for a human (H) and vehicle (V) target scenario for varying SINRs. Notice that for all SINR levels the algorithm correctly classifies the vehicle, but that as the SINR decreases, the number of trials in which the human is mistakenly classified increases.

TABLE III

SINR			ACTUAL H	ACTUAL V
PREDICTED	20 dB	H	100	0
		V	0	100
	0 dB	H	100	0
		V	0	100
	-5 dB	H	43	0
		V	57	100
	-10 dB	H	3	97
		V	0	100
	-20 dB	H	0	0
		V	100	100

VI. CONCLUSION

The proposed human modeling-based, non-linear phase detectors, ONLP and EnONLP, both outperform conventional linear-phase detectors. EnONLP can be used not only for detecting human targets, but for detection and classification of targets of any type, including animals, just so long as the appropriate model is included in the dictionary. Estimates of the model parameters yielded by the EnONLP algorithm may be also used to extract additional information about detected targets.

REFERENCES

[1] M. Otero, "Application of a continuous wave radar for human gait recognition," *in Proc. SPIE*, Vol. 5809, pp. 538-548, 2005.

[2] S.Z. Gürbüz, W.L. Melvin, and D.B. Williams, "Detection and Identification of Human Targets in Radar Data," *in Proc. SPIE*, Orlando, FL, April 9-13, 2007.

[3] S.Z. Gürbüz, W.L. Melvin, and D.B. Williams, "Comparison of Radar-Based Human Detection Techniques," *in 41st Asilomar Conf.*, Monterey, CA, November 4-7, 2007.

[4] S.Z. Gürbüz, W.L. Melvin, and D.B. Williams, "A Non-Linear Phase, Model-Based Human Detector for Radar, "accepted for publication, *IEEE Trans. AES.*

[5] R. Boulic, M.N. Thalmann, and D. Thalmann, "A Global Human Walking Model with Real-Time Kinematic Personification," *Vis. Comp*. Vol. 6, pp. 344-358, 1990.

[6] J.L. Geisheimer, E.F. Greneker, and W.S. Marshall, "A high-resolution Doppler model of human gait," *in Proc. SPIE*, Vol. 4774, 2002.

[7] P. Van Dorp, and F.C.A. Groen, "Feature-Based Human Motion Parameter Estimation with Radar," IET Radar, Sonar, and Navigation, Vol. 2, Issue 2, pp. 135-145, April 2008.

[8] F.C. Robey, D.R. Fuhrman, E.J. Kelly, and R. Nitzberg, "A CFAR Adaptive Matched Filter Detector," *IEEE Trans. AES*, Vol. 28, No. 1, January 1992.

[9] J.A. Tropp, "Topics in Sparse Approximation," PhD Diss., The University of Texas at Austin, August 2004.